OPTOELECTRONICS AND ADVANCED MATERIALS – RAPID COMMUNICATIONS Vol. 4, No. 10, October 2010, p. 1542 - 1545

Synthesis, characterization and optical properties of Ni-doped nanocrystalline SnO_2

L. S. CHUAH[*], M. Y. YAACOB, M. S. FAN, S. S. TNEH[a], Z. HASSAN[a]
Physics Section, School of Distance Education, Universiti Sains Malaysia, 11800 Penang, Malaysia
[a]School of Physics, Universiti Sains Malaysia, 11800 Penang, Malaysia

Sol–gel processing is a simple way of preparing chemically homogeneous, high-purity and phase-pure powders at a lower temperature. Nanometer-scale SnO_2 particles have been synthesized by a simple sol–gel method. Tin oxide nanoparticles were prepapred by the sol-gel route. In a typical synthesis, a 0.05 M tin(II) chloride ($SnCl_4.2H_2O$) in deionized water was prepared and was added in 100 ml ethanol, to get equal proportions of water and ethanol, and then ultrasonic bath for 10 min. Followed by 1.5 wt % $NiCl_2.6H_2O$, Nickel chloride-6-hydrate was added as the doped source into previous solution, and then ultrasonic bath for 5 min. The coatings were prepared by spin coating the preceding solutions at 500 rpm onto glass substrates. The coating process was repeated five times. After spinning, the sample was placed on the substrate holder inside tubular furnace. Then, the samples were dried in air at 100, 200, 300, 400, 500, 600 and 700 °C for 30 min, respectively, in an electrically heated furnace. The samples were characterized by Fourier transform infrared (FTIR) spectroscopy. It is noteworthy that, no diffraction peaks corresponding to Ni oxides such as NiO are detected.

(Received September 2, 2010; accepted October 14, 2010)

Keywords: Nanocrystalline SnO_2 thin films, Band gap energy, FTIR spectroscopy

1. Introduction

Tin oxide (SnO_2) is an n-type wide band gap (3.6-3.8 eV) semiconductor and it had been used in a variety of applications such as gas sensors for gas mixture; transparent conductive films for solar cells; optoelectronic devices; electrode materials; lithium batteries; and catalysts for the oxidation of organic compounds [1-3]. The interesting characteristics and related pplications were dominated by several factors, such as morphology, grain size, crystallinity and etc [4].

In recent years, nanocrystalline particles with a high surface area showed improved properties in gas sensing for example. Synthesis of nanomaterials with well controlled size, morphology and chemical composition may open new opportunities in exploring newand enhanced physical properties. The microstructure of SnO_2 could be controlled by temperature treatment, doping and method of preparation [5-7].

SnO_2 nanoparticles can by synthesized using a various methods for example RF magnetron sputtering, electron beam evaporation, high energy ball milling method; homogeneous precipitation; chemical vapor deposition; hydrothermal; solvothermal; microemulsion; sol–gel coating; spray pyrolysis; polymerized complex citrate route; and non-aqueous approaches [8-10].

In a literature review, Cheng and Chan studied antimony doping of tin dioxide as a novel anodic material for ozone electrolytic generation. They have been reported high current efficiency and high dissolved ozone concentration at room temperature [11]. Furthermore, due to our goal was the development of gas sensor devices, the SnO_2 sols were doped with nickel. Ordinarily, dopants are applied as catalysts in the fabrication of gas sensor for obtaining a faster response of the device and for making it more selective toward a given gas. The doping modifies the electronic structure of the material, which can cause more effective electron-hole pair generation that is especially significant for utilizations that are based on light-induced phenomena.

The above considerations make it important to study the influence of doping on the properties of sol-gel derived SnO_2. In this paper, optical properties of sol-gel process nanocrystalline Ni-doped SnO_2 thin films have been studied in post thermal annealed (in air over the temperature range of 100 °C – 700 °C) conditions using Fourier transform infra-red spectroscopy (FTIR).

2. Experimental

Tin oxide nanoparticles were prepapred by the sol-gel route. In a typical synthesis, a 0.05 M tin(II) chloride ($SnCl_4.2H_2O$) in deionized water was prepared and was added in 100 ml ethanol, to get equal proportions of water and ethanol, and then ultrasonic bath for 10 min. Followed by 1.5 wt % $NiCl_2.6H_2O$, Nickel chloride-6-hydrate was added as the doped source into previous solution, and then ultrasonic bath for 5 min.

The coatings were prepared by spin coating the preceding solutions at 500 rpm onto glass substrates. The coating process was repeated five times. After spinning, the sample was placed on the substrate holder inside tube furnace (Fig. 1). Then, the samples were dried in air at 100, 200, 300, 400, 500, 600 and 700 °C for 30 min, respectively, in an electrically heated furnace. The samples were characterized by Fourier transform infrared (FTIR) spectroscopy.

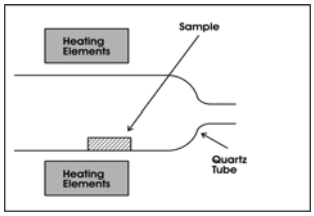

Fig. 1. Setup of tube furnace for thermal annealing.

The schematic diagram of a Michelson interferometer is shown in Fig. 2. The light source is first collimated by a collimator mirror before being directed at a beam splitter, positioned at 45^o to the incident beam. A KBr beamsplitter separates the beam into two beams, each having amplitude of half the original beam and propagates at right angles to each other [12]. One of the beams reflects off a movable mirror while the other beam reflects off a fixed mirror. The two beams then recombine at the beamsplitter, and the superposition of the beams is a function of the displacement of the movable mirror, which controls the optical path difference [13]. The mirror displacement is measured in reference to the zero point position, for example the point where the distance from the fixed mirror and the movable mirror to the beam spitter is equal. The continuous spectrum of the IR source can be considered as being composed of many monochromatic beams, each of different frequencies. These component beams are all completely in phase with each other only at the zero point position. At this point, constructive interference occurs, resulting in a maximum signal known as centre burst in the interferogram [14].

The resulting beam is then reflected off an adjustable focusing mirror to the sample at a near-normal incidence angle of 30^o. The light incident on the sample is partly absorbed while the remainder is reflected from the sample and directed to the detector. Data acquisition is performed at a data interval of 1cm^{-1}. The interferogram is then digitized and fed to the computer where Fourier transform is performed. Since the spectrum obtained consists of the contribution from both the sample and the instrument (background), background correction must be carried out to eliminate the background contribution. This is achieved by ratioing the spectrum of the sample to the background (in the absence of the sample) spectrum. The spectrum obtained after the ratio is called the reflectance spectrum. This is the spectrum that will be used for data analysis.

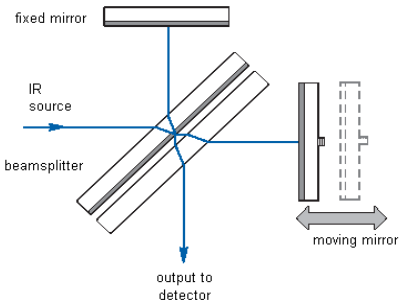

Fig. 2. Schematic of a generic Michelson interferometer.

3. Results and discussion

FTIR spectroscopy is a non-destructive technique which, although is most commonly associated with chemical identification, has also proven to be useful for optical characterization of semiconductor thin films. For SnO_2, IR studies have been conducted on bulk SnO_2. In recent years, FTIR spectroscopy has also been applied to SnO_2 epilayers and structures. For this work, FTIR spectroscopy was employed to obtain the optical spectrum of the samples in the reststrahlen region of SnO_2 (~ 400 – 4000 cm^{-1}) and analyzed to study its optical properties. FTIR spectroscopy can also be used to determine phonon modes and is usually regarded as a complementary technique to Raman spectroscopy.

In IR spectroscopy, the sample is irradiated with IR radiation, where part of the radiation is absorbed and inducing vibrionic excitation. The remainder of the radiation is then transmitted or reflected to a detector. One of the most frequently used methods in FTIR spectroscopy employs two-beam interferometers such as the Michelson interferometer. The Michelson interferometer works on the principle that when two beams combine, interference occurs in accordance to their optical path difference. The intensity of the resultant beam as a function of optical path difference is called the interferogram. The interferometer first collects the interferogram. Then, with the aid of a computer, the interferogram is converted to the optical spectrum, i.e. intensity as a function of frequency/wavenumber, by performing a mathematical analysis called the Fourier Transform.

Using a Perkin Elmer Spectrum GX Michelson interferometer, room temperature measurements were conducted on the samples. The interferometer has interchangeable optics and is capable of conducting both mid and far IR measurements. For this study, the region of interest is the reststrahlen region of SnO_2 which falls in the mid-IR region. The Kramers-Kronig analysis is then performed on the reflectance spectra to obtain the phase, optical and dielectric constants as a function of wavenumber, and finally the optical phonon frequencies of the sample.

Fig. 3 shows the FTIR patterns of the as-deposited specimen and the samples heat-treated from 100 °C to 700 °C for 30 min, respectively. Tin oxide FTIR pattern generally shows the presence of stretching vibration bands at around 540 cm^{-1}. The peak at 800 cm^{-1} can be assigned to Sn-O-Sn stretching vibrations. The absorption band at 540 cm^{-1} was ascribed to the the terminal oxygen vibration (Sn-OH). A broad band around 3500 cm^{-1}, coupled to that at about 1640 cm^{-1}, characteristic of water bending, is observed in the as-deposited, 100 °C and 200 °C sample. For sample annealed at 300 °C, 400 °C, 500 °C, 600 °C, and 700 °C, the absorption observed at 1640 cm^{-1} due to OH group is weak or absent. In all the samples, absorption peaks near 550 cm^{-1} corresponding to Sn-O vibrations, was observed. The disappearance of bands around 3500 cm^{-1} when the sample is heat-treated at 700 °C for 30 min confirms the elimination of hydroxyl groups in our densified samples. No additional absorption peaks were

observed with Ni addition, indicating its homogeneous dispersion in the support material.

Popescu and Verduraz et al. [15] have seen these peaks for SnO_2 powder at 665 cm^{-1}, 770 cm^{-1} and 960 cm^{-1}, respectively; their peaks were comparatively narrower in comparison with our FTIR spectra. This may be due to amorphous and nanocrystalline nature of our films. The shape of the FTIR spectra and the positions of the peaks have been shown to vary with the synthesis routes and particle size [16].

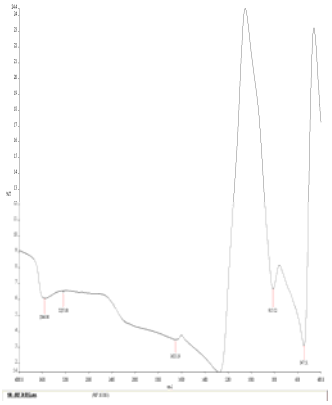

(a) 100 °C

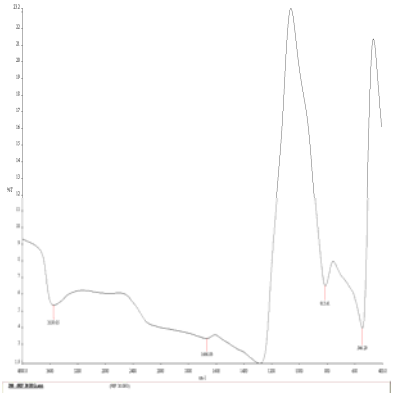

(b) 200 °C

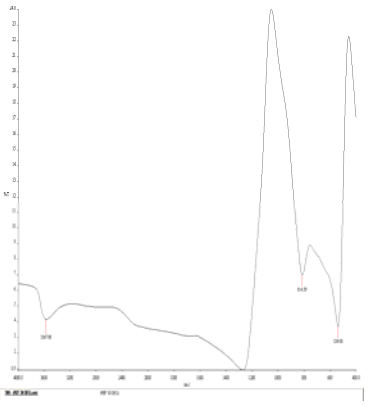

(c) 300 °C

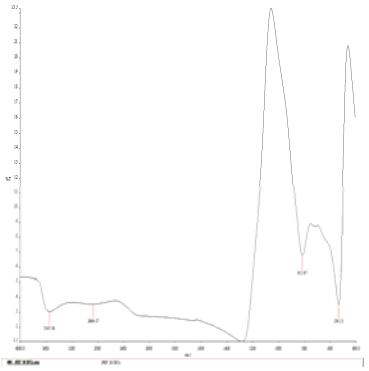

(d) 400 °C

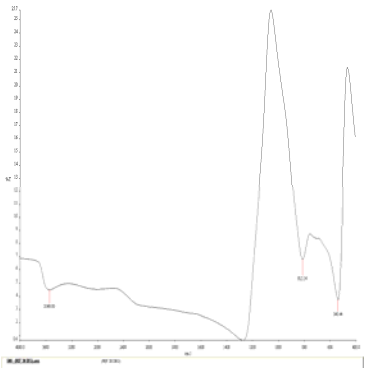

(e) 500 °C

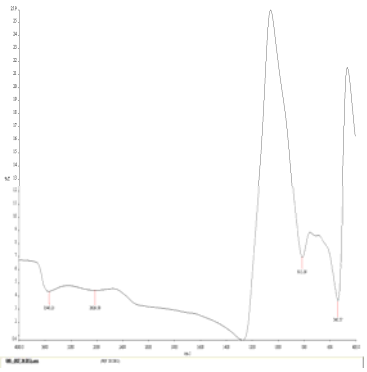

(f) 600 °C

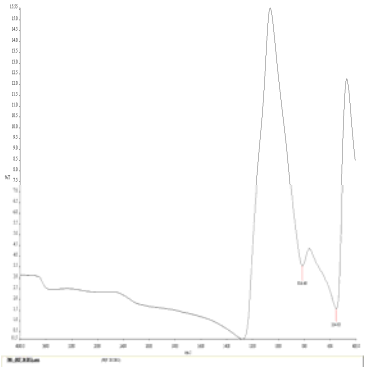

(g) 700 °C

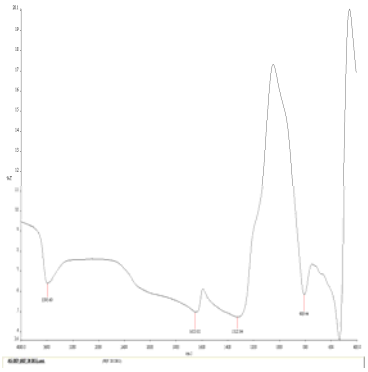

(h) As deposited

Fig. 3. The FTIR patterns of the as-deposited specimen and the samples heat-treated from 100 °C to 700 °C for 30 min.

4. Conclusions

In conclusion, SnO_2 nanoparticles have been successfully prepared by a simple sol–gel method. FTIR spectra of the samples have also been investigated. Tin oxide FTIR pattern generally shows the presence of stretching vibration bands at around 540 cm^{-1}. The peak at 800 cm^{-1} can be assigned to Sn-O-Sn stretching vibrations. The absorption band at 540 cm^{-1} was ascribed to the the terminal oxygen vibration (Sn-OH). A broad band around 3500 cm^{-1}, coupled to that at about 1640 cm^{-1}, characteristic of water bending, is observed in the as-deposited, 100 °C and 200 °C sample. For sample annealed at 300 °C, 400 °C, 500 °C, 600 °C, and 700 °C, the absorption observed at 1640 cm^{-1} due to OH group is weak or absent. In all the samples, absorption peaks near 550 cm^{-1} corresponding to Sn-O vibrations, was observed. The disappearance of bands around 3500 cm^{-1} when the sample is heat-treated at 700 °C for 30 min confirms the elimination of hydroxyl groups in our densified samples.

Acknowledgement

The authors would like to acknowledge the Universiti Sains Malaysia for financial assistance through a Short Term Grant.

References

[1] R. Adnan, N. A. Razana, Ismail Abdul Rahman, M. A. Farrukh, Journal of the Chinese Chemical Society, **57**, 222 (2010).
[2] A. Cirera, A. Vila, A. Cornet, J. R. Morante, Materials Science and Engineering **C15**, 203 (2000).
[3] Abhilasha Srivastava, S. T. Lakshmikumar, A. K. Srivastava, Kiran Jain Rashmi, Sensors and Actuators B **126**, 583 (2007).
[4] Arunkumar Lagashetty, A. Venkataraman, Bulletin Materials Science **2**, 491 (2004).
[5] Ki Chang Song, Yong, Kang, Materials Letters **42**, 283 (2000).
[6] A. Cobot, J. Arbiol, J. R. Morante, U. Weimar, N. Barsan, W. Gopal, Sensors and Actuators B **70**, 87 (2000).
[7] A. M. Azad, S. A. Akbar, S. G. Mhaisalkar, L. D. Birkeffeld, K. S. Goto, Journal of the Electrochemical Society **139**, 3690 (1992).
[8] Z. Z. You, J. Y. Dong, Microelectron. J. **38**, 108 (2007).
[9] J.-S. Lim, P.-K. Shin, Appl. Surf. Sci. **253**, 2828 (2007).
[10] S. Rani, S. C. Roy, M. C. Bhatnagar, Sens. Actuators B: Chem. **122**, 204 (2007).
[11] S. A. Cheng, K. Y. Chan, Electrochem. Solid-State Lett., **7**, D4 (2004).
[12] Antoine Abragam. 1968. Principles of Nuclear Magnetic Resonance, Cambridge University Press: Cambridge, UK.
[13] Peter Atkins, Julio De Paula, 2006, Physical Chemistry, 8th ed. Oxford University Press: Oxford, UK.
[14] M. J. Mattu, G. W. Small, Anal. Chem. **67**, 2269 (1995).
[15] D. A. Popescu, F. B. Verduraz, Catal. Today **70**, 139 (2001).
[16] M. Ristic, M. Ivanda, S. Popovic, S. Music, J. Non-Crystall. Solids **303**, 270 (2002).

*Corresponding author: chuahleesiang@yahoo.com